Qian Wu[1]
Xinwei Yu[1]
Yan Wang[1]
Xue Gu[1]
Xiaoqiong Ma[2]
Wang Lv[2]
Zhe Chen[2]
Chao Yan[1]

[1]School of Pharmacy, Shanghai Jiao Tong University, Shanghai, China
[2]Zhejiang Provincial Hospital of Traditional Chinese Medicine, Zhejiang Chinese Medical University, Hangzhou, China

Received March 9, 2014
Revised April 19, 2014
Accepted April 19, 2014

Research Article

Pressurized CEC coupled with QTOF-MS for urinary metabolomics

Pressurized CEC (pCEC) coupled with ESI-QTOF-MS using a sheathless interface was applied for metabolomics to develop an alternative analytical method for metabolic profiling of complex biofluid samples such as urine. The hyphenated system was investigated with mixed standards and pooled urine samples to evaluate its precision, repeatability, linearity, sensitivity, and selectivity. The applied voltage, mobile phase, and gradient elution were optimized and applied for the analysis of urinary metabolites. Multivariate data analysis was subsequently performed and used to distinguish lung cancer patients from healthy controls successfully. High separation efficiency has been achieved in pCEC due to the EOF. For metabolite identification, the pCEC-MS separation mechnism was helpful for discriminating the fragment ions of glutamine conjugates from co-eluted metabolites. Three glutamine conjugates, including phenylacetylglutamine, acylglutamine C8:1, and acylglutamine C6:1 were identified among 16 differential urinary metabolites of lung cancer. Receiver-operating-characteristic analysis of acylglutamine C8:1 resulted in an area-under-curve value of 0.882. Overall, this work suggests that this pCEC-ESI-QTOF-MS method may provide a novel and useful platform for metabolomic studies due to its superior separation and identification.

Keywords:
Glutamine conjugates / Lung cancer / Metabolomics / Pressurized CEC-MS / Urine
DOI 10.1002/elps.201400117

Additional supporting information may be found in the online version of this article at the publisher's web-site

1 Introduction

CEC is a hybrid separation technique that combines capillary HPLC (cHPLC) and CE [1]. Therefore, CEC has both the high selectivity and peak capacity of HPLC and the high efficiency and resolution of CE. CEC is capable of separating both neutral and charged substances. However, CEC also has problems, such as bubble formation caused by Joule heating during experiments, which can result in column dryout and current disruption. Therefore, pressurized CEC (pCEC) or pressure-assisted CEC (pCEC), with EOF combined with supplemental pressurized flow as its driving force, has been used to overcome these problems [2]. pCEC has several other advantages: (i) high separation efficiency and resolution through its small particle-packed column, (ii) high selectivity with a dual separation mechanism, (iii) quantitative sample injection with a rotary-type valve, and, most importantly, (iv) a high pressure gradient elution similar to that in HPLC [3].

MS provides highly sensitive and selective, molecular weight and structural information. Moreover, it offers both qualitative and quantitative information of peptides or metabolites in complex samples such as biological fluids. MS combined with chromatography is a key analytical technique in emerging "omics" technologies such as proteomics, metabolomics, and lipidomics [4]. In addition, the low flow rate of pCEC is highly compatible with an ESI source, and the coupling of pCEC with MS combines the merits of pCEC and MS.

The pCEC-MS analysis depends on the interface used to provide a return path for both the CEC column and electrospray current, as the length of the interface and its structure can greatly affect separation results. So far, three main kinds of interfaces [5], sheathless [6, 7], liquid-junction [8, 9], and

Correspondence: Professor Chao Yan, School of Pharmacy, Shanghai Jiao Tong University, 800 Dongchuan Road, Shanghai 200240, China
E-mail: chaoyan@unimicrotech.com
Fax: +86-21-38953636

Abbreviations: cHPLC, capillary HPLC; **FA**, formic acid; **PAGN**, phenylacetylglutamine; **PCA**, principal component analysis; **pCEC**, pressurized CEC; **QC**, quality control; **VIP**, variable importance in projection

Colour Online: See the article online to view Figs. 1, 3, and 4 in colour.

coaxial sheath liquid [10–13] have been constructed for CEC-ESI-MS coupling.

CE-MS has been widely applied in the analysis of metabolomics [14–17] for biological samples because it has proven suitable for the profiling of polar and charged metabolites. A combination of CEC-MS and LC-MS, pCEC-MS has been successfully applied in the analysis of peptides, proteins [18–23], and drugs abuse [9, 24–27]. However, to date, pCEC-MS has not been reported for applications in metabolomics, although CEC-MS has been used for targeted screening in human plasma [28] and bile acids in animal bile [29], and open tubular CEC-MS has been developed to analyze the metabolome of a cell line [30]. Another technique using pCEC, pCEC-UV, has been applied for the metabolic profiling of rat urine [31] and human plasma [32], confirming that pCEC has a great potential in metabolomic research. However, since a UV detector cannot provide structural information of metabolites, it is not ideal for the identification of disease biomarkers.

In this study, pCEC coupled with QTOF MS was applied for metabolomics for the first time to develop an alternative analytical method for metabolic profiling. A sheathless interface was constructed for MS coupling, operation parameters optimized, and system repeatability evaluated for isocratic and gradient elution. The gradient pCEC-QTOF-MS method was then used to analyze urinary metabolites in lung cancer patients.

2 Materials and methods

2.1 Reagents and materials

Formic acid (FA) and sodium formate were obtained from CNW (Düsseldorf, Germany). HPLC grade ACN and methanol were purchased from Merck (Darmstadt, Germany). Water was purified with a Barnstead Nanopure purification system (Dubuque, IA, USA). L-2-Chlorophenylalanine was purchased from Intechem Tech. (Shanghai, China). All other standards were purchased from Sigma-Aldrich (St. Louis, MO, USA).

2.2 Hyphenation of pCEC with ESI-QTOF-MS

A schematic of the pCEC-MS on-line system is shown in Fig. 1. Chromatographic separation was performed on a reversed-phase column (EP-150–25/25–5-C18, Global Chromatography, Suzhou, China) of 25 cm (of which 25 cm was packed) × 150 μm id packed with 5 μm C18 particles using the TriSep-2100 pCEC system (Unimicro Technologies, Pleasanton, CA, USA) consisting of a high-pressure micro-LC pump, a six-port injection valve, a four-port split valve, a high voltage power supply ±30 kV, and a self-made capillary flow-cell holder.

The solvent delivery system was used to provide supplementary pressure and deliver a solvent gradient at a typical flow rate of 0.08 mL/min. Samples were injected into an external sample loop and then carried by the mobile phases to the four-port split valve. After splitting in the four-port valve, the flow entered the capillary column. The inlet of the column was connected to the four-port split valve, with a positive or negative voltage applied, and the column outlet was connected to the mass electrospray with a zero dead volume stainless steel union and grounded. To avoid high voltage, both pumps were grounded as well.

For pCEC-MS system performance experiments, the sample injection volume was 35 nL for each scan (2.4 μL loop, split ratio 68:1). Binary solvents of A (0.1% FA in 2% ACN, v/v) and B (0.1% FA in 98% ACN, v/v) were used in isocratic elution. For the metabolomic and MS/MS experiments, the sample injection volume was 147 nL for each scan (10 μL loop, split ratio 68:1). Binary solvents of A (0.1% FA in 2% ACN, v/v) and B (1% FA in ACN–methanol–water 49:49:2, v/v/v) were used in gradient elution. For gradient elution, sampling stacking [19] was performed as follows. First, the sample solution was introduced into the column by the propelling force of the mobile phase. Second, after a certain

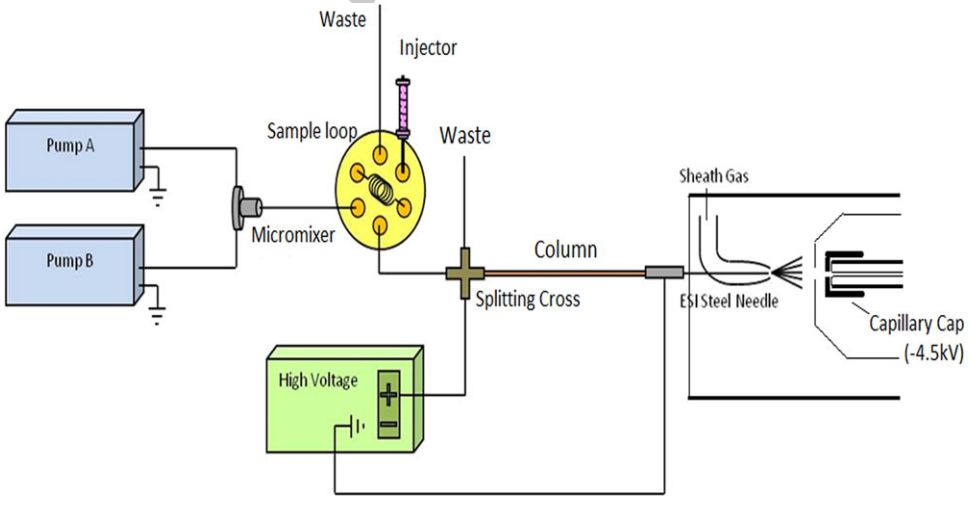

Figure 1. Schematic diagram of pCEC coupled with ESI-MS.

period of on-column stacking, the voltage was added to the separation voltage in 10 s. The stacking time was optimized as 4 min for final urine analysis.

The pCEC system was coupled to the ESI source of a high-resolution mass spectrometer (maXis UHR-TOF, Bruker Daltonics, Bremen, Germany). The ion polarity was positive and the capillary voltage was 4500 V. The end plate offset potential was set at −500 V. The dry gas was set as 4 L/min at 180°C. The nebulizer gas pressure was set at 0.4 bar. Mass spectra were acquired in the full-scan mode in the range of 50–1000 Da. One millimolar sodium formate in isopropanol–water (50:50, v/v, with 0.2% FA) was used as calibrating solution via direct infusion. MS/MS experiments were performed under the auto-MS/MS mode with a range of collision energy from 20 to 35 eV.

2.3 Sample collection and preparation

Urine samples were obtained from Zhejiang Provincial Hospital of Traditional Chinese Medicine (Hangzhou, China). Informed consent was obtained from all patients and volunteers, and approval was obtained from the local research ethics committee. The lung cancer patients ($n = 12$; mean age 57 ± 12 years; six males and six females) were diagnosed through magnetic resonance imaging and then histologically proven to have lung cancer. The urine samples from patients were collected before medical treatments or surgery. The healthy volunteers ($n = 12$; mean age 55 ± 10 years; six males and six females) were selected by a routine physical examination. Detailed clinical information of urine samples is provided in Supporting Information Table S1. There was no significant difference for age and sex ratio between lung cancer patients and healthy controls. The p-value of Student's t-test for age between the two groups was 0.71. All urine samples were collected in the morning before breakfast. The samples were centrifuged at 4°C at 3000 rpm for 15 min and stored at −80°C until use.

Each 100 μL urine sample was mixed into 100 μL L-2-chlorophenylalanine (10 μg/mL), vortexed for 1 min, and then centrifuged at 13 000 rpm for 15 min at room temperature. The supernatant was transferred into a clean tube and stored at 4°C before analysis. For quality control (QC), a pooled "QC" sample was prepared by mixing 100 μL from each of the healthy control samples. The QC samples were also used in the optimization of separation and MS conditions.

2.4 Data pretreatment and statistical analysis

The raw data were acquired on a micrOTOFcontrol workstation (Bruker Daltonics) and then converted into NetCDF format by DataAnalysis version 3.3 (Bruker Daltonics). The NetCDF format data were analyzed by the MarkerLynx Applications Manager version 4.1 (Waters, Manchester, UK) using the following parameters: retention time range 1–40 min, mass range 50–1000 Da, mass tolerance 0.05 Da, intensity threshold at 500 counts, isotopic peaks excluded for analysis, and retention time window set at 1.00 min. Data were imported to the SIMCA-P 11.5 demo version (Umetrics, Umeå, Sweden) for further analysis. Principal component analysis (PCA) and orthogonal partial least squares-discriminant analysis were carried out to visualize metabolic alterations and Pareto scaling was used. The variable-importance-in-projection (VIP) values and S-plot were selected to obtain the significant variables [33, 34]. The Student's t-test was selected to measure the significance of each variable. Variables with VIP > 1 and $p < 0.05$ were considered differential metabolites. The Mann–Whitney U test was subsequently applied to confirm the significance.

3 Results and discussion

3.1 Comparison of different interfaces

Three different kinds of interfaces were tested in this study (Fig. 2). The supplementary liquid interface (Fig. 2A) used a PEEK cross to combine the separation column, the supplementary liquid flow, and the grounding electrode. The supplementary liquid was 0.1% FA in 50% ACN v/v and the flow rate was 180 μL/h. The nonsupplementary liquid interface (Fig. 2B) removed the inlet of the supplementary liquid, significantly avoiding sample dilution. However, the removal of supplementary liquid may cause instability and peak inversion because the PEEK tube between the separation column and the spray needle was not fixed. The sheathless interface (Fig. 2C) was developed from the above two interfaces. It was able to reduce the impact from the external environment with a fixed capillary column. The sheathless interface was used for further experiments because it reduced peak broadening, improved peak shape, and performed the best separation compared to the other two interfaces (Fig. 2D).

3.2 Evaluation of the sheathless interface under isocratic conditions

The flow rate was optimized for the sheathless interface. The interface was then evaluated for the analysis of spiked standards consisting of several representative endogenous urinary metabolites and an internal standard under isocratic elution conditions.

The relatively higher flow rates (1–2 μL/min) provided by packed capillary columns with large internal diameters (150 μm) permit the use of conventional ESI source without sheath liquid. The higher flow rate can improve the MS signal response and shorten the analysis time while column pressure significantly grows. The pump flow rate tested ranged from 0.06 to 0.10 mL/min (0.06, 0.08, and 0.10 mL/min, respectively). Other parameters were the same as in Fig. 2 except that an isocratic elution (10% B) was applied. A pump flow rate of 0.08 mL/min gave a tolerable pressure (15 MPa) and acceptable signal intensity (1.5×10^5, baseline), and was used for further experiments.

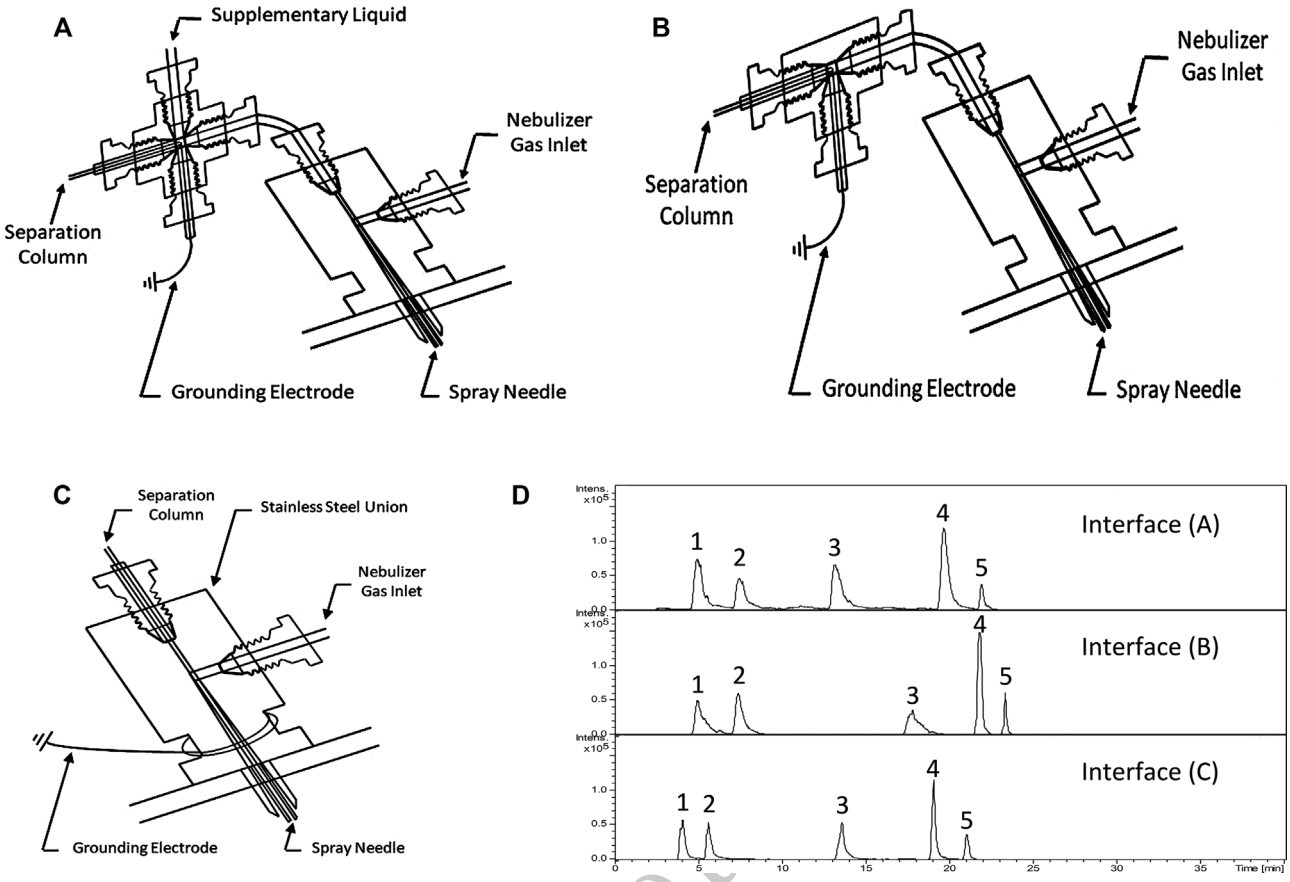

Figure 2. Schematic diagrams of different interfaces (A) supplementary liquid, (B) nonsupplementary liquid, (C) sheathless, and (D) their corresponding chromatograms. pCEC conditions: column, 25 cm × 150 μm, C18, 5 μm; mobile phase A, 0.1% FA in 2% ACN v/v; mobile phase B, 0.1% FA in 98% ACN v/v; gradient, 0–30 min 0–50% B, 30–40 min 50–100% B; flow rate, (A) 0.06 mL/min + 180 μL/h supplementary liquid, (B) and (C) 0.08 mL/min; injection volume, 35 nL; applied voltage, 0 kV. Sample: 1, histidine; 2, nicotinamide; 3, phenylalanine; 4, L-2-chlorophenylalanine; 5, hippuric acid. MS conditions: spray voltage, 4.5 kV; dry gas, 4 L/min, 180°C; nebulizer gas, 0.4 bar.

The repeatability of the sheathless interface was investigated with isocratic elution under three hyphen patterns (Supporting Information Table S2). Acceptable repeatability of retention times was observed, with RSD values ranging from 0.17 to 2.84%. The variation of peak intensity was found to be broadly acceptable, with RSD values ranging from 3.26 to 13.54%. The above results showed that the developed pCEC-MS system had a reasonably good repeatability under isocratic elution mode.

3.3 Optimization of operation parameters for the urine sample

3.3.1 Optimization of mobile-phase composition

Urine contains both polar (or ionizable) metabolites and nonpolar lipids with a wide range of lipophilicity [35], thus posing a real challenge to separation technology. The ionic strength, composition, and concentration of acid modifiers in the mobile phase greatly impact elution capacity. Separation generally increases with higher ionic strength of the mobile phase solution, while the loss of MS signal intensity often occurs. In this study, 0.1% FA in 2% ACN v/v was used as mobile phase A, and three kinds of mobile phase B were investigated (0.1% FA in 2% ACN, v/v; 0.1% FA in ACN–methanol–water 49:49:2, v/v/v; and 1% FA in ACN–methanol–water 49:49:2, v/v/v, respectively; Supporting Information Fig. S1). The 0.1% FA in 2% ACN v/v / 1% FA in ACN–methanol–water 49:49:2 v/v/v gradient system had the best peak shape and resolution, and was conducive to the elution of strong retention substances; therefore, it was used for further experiments.

3.3.2 Effect and optimization of applied voltage

The separation voltage greatly affects the EOF, which drives the mobile phase toward the detection end of the capillary column. The influence of applied voltage on the separation of the analytes was therefore evaluated (Supporting Information Fig. S2). The separation of the spiked standards significantly changed, and a shorter analysis time achieved, with increasing voltage. Due to EOF and electrophoretic mobility, when different voltages were applied, the retention times, the resolution of the analytes, and even the elution order of

L-2-chlorophenylalanine and tryptophan were changed. These results demonstrated the selectivity of the pCEC-MS system. However, higher voltage resulted in system instability due to the unwanted Joule heating caused by the increased current. Based on these results, a +12 kV separation voltage was adopted for further urine analysis.

3.3.3 Comparison of pCEC, cHPLC, and HPLC

The urine samples were examined in three different separation modes. The number of molecular features found in pCEC, cHPLC, and conventional HPLC coupled with MS was 978, 510, and 731, respectively, under the same S/N (S/N = 10, Supporting Information Table S3). As illustrated in Supporting Information Fig. S3, more molecular features were extracted in pCEC-MS compared to cHPLC-MS under the same MS conditions, due to reduced peak width from the EOF and additional selectivity from electrophoretic migration. High separation efficiency indicated the value of pCEC-MS for metabolomic studies.

3.3.4 Optimization and validation of gradient elution

Compared to the traditional CEC-MS system, the pCEC-MS system is advantageous as the multipump of pCEC can achieve gradient elution. Therefore, several gradient elution conditions were investigated. The results showed the best gradient elution condition (0–20 min 0–20% B, 20–25 min 20–100% B, 25–30 min 100% B), which exhibited good peak shape, resolution, and sensitivity. This condition was used for further experiments.

Five independent samples were prepared from one QC sample and injected respectively to study reproducibility with respect to retention time and peak area. The results for seven common peaks selected to cover a wide range of retention time and *m/z* are shown in Supporting Information Table S4. The obtained data indicated that the RSD values ($n = 5$) were better than 2.17% for retention times and ranged from 5.36 to 10.83% for peak areas. The above results demonstrated the acceptable repeatability of the established method in real sample analysis.

The linearity and LODs were investigated with spiked standards and calculated by extracted ion chromatograms. A series of mixed standards solutions of different concentrations consisting of histidine, nicotinamide, tyrosine, phenylalanine, L-2-chlorophenylalanine, and hippuric acid were analyzed. Table 1 shows that linearity calibration curves were obtained in the concentration range 0.1–500 μg/mL for different compounds with correlation coefficients from 0.9956 to 0.9985. The LODs for the test compounds were between 18 and 88 ng/mL with the S/N values ranging from 7 to 30 (Table 1). To further evaluate the matrix effect, each 50 μL aliquot of 10, 50, and 100 μg/mL of the spiked standards solution was added to 50 μL pooled urine sample (final concentration of 5, 25, and 50 μg/mL). The matrix effect was calculated using the following equation [36]:

$$\text{matrix effect}\,(\%) = \frac{B - A - C}{C} \times 100\% \quad (1)$$

where C is the peak area of standard spiked into water (v/v = 1:1), B is the peak area of standard spiked into a pooled urine sample (v/v = 1:1), and A is the corresponding peak area of the endogenous metabolite in urine sample spiked into water (v/v = 1:1). The results, as shown in Table 1, indicated that matrix effect was evident in human urine matrix with values ranging from −8.4 to −34.7% in most cases. The matrix effect of histidine was an exception due to its co-elution with some abundant metabolites such as creatinine.

3.4 Metabolic profiles between lung cancer patients and healthy controls

pCEC-MS was applied in the metabolic profiling of urine samples from lung cancer patients and healthy controls. After washing the system with several blank samples, QC samples were injected repeatedly for conditioning. One blank sample and one QC sample were injected in order before every eight samples. Line plots of three QC samples during the analysis using PCA with all the points in 2 SD regions demonstrate the stability of the system (Supporting Information Fig. S4).

After data normalization, PCA was performed on the dataset, which showed a trend of separation between the two groups (data not shown). Figure 3A–B shows the scores

Table 1. Linearity, LOD, and matrix effect obtained by pCEC-MS using a sheathless interface

Compound	Linearity			LOD		Matrix effect[b] ($n = 5$)		
	Range (μg/mL)	N[a]	R^2	LOD (ng/mL)	S/N	5 μg/mL (mean,%)	25 μg/mL	50 μg/mL
Histidine	0.1–100	7	0.9956	20	28	−97.2	−96.7	−97.1
Nicotinamide	0.1–100	7	0.9985	20	12	−13.6	−8.4	−9.7
Tyrosine	0.5–100	6	0.9977	88	13	−34.7	−24.3	−24.7
Phenylalanine	0.1–100	7	0.9972	18	11	−13.8	−10.2	−11.4
L-2-Chlorophenylalanine	0.1–50	6	0.9985	22	30	−16.6	−10.7	−14.6
Hippuric acid	0.5–500	7	0.9971	40	7	−27.7	−28.5	−23.6

a) *N* means an *N*-point calibration curve over the range.
b) Matrix effect was calculated from spiked urine samples.

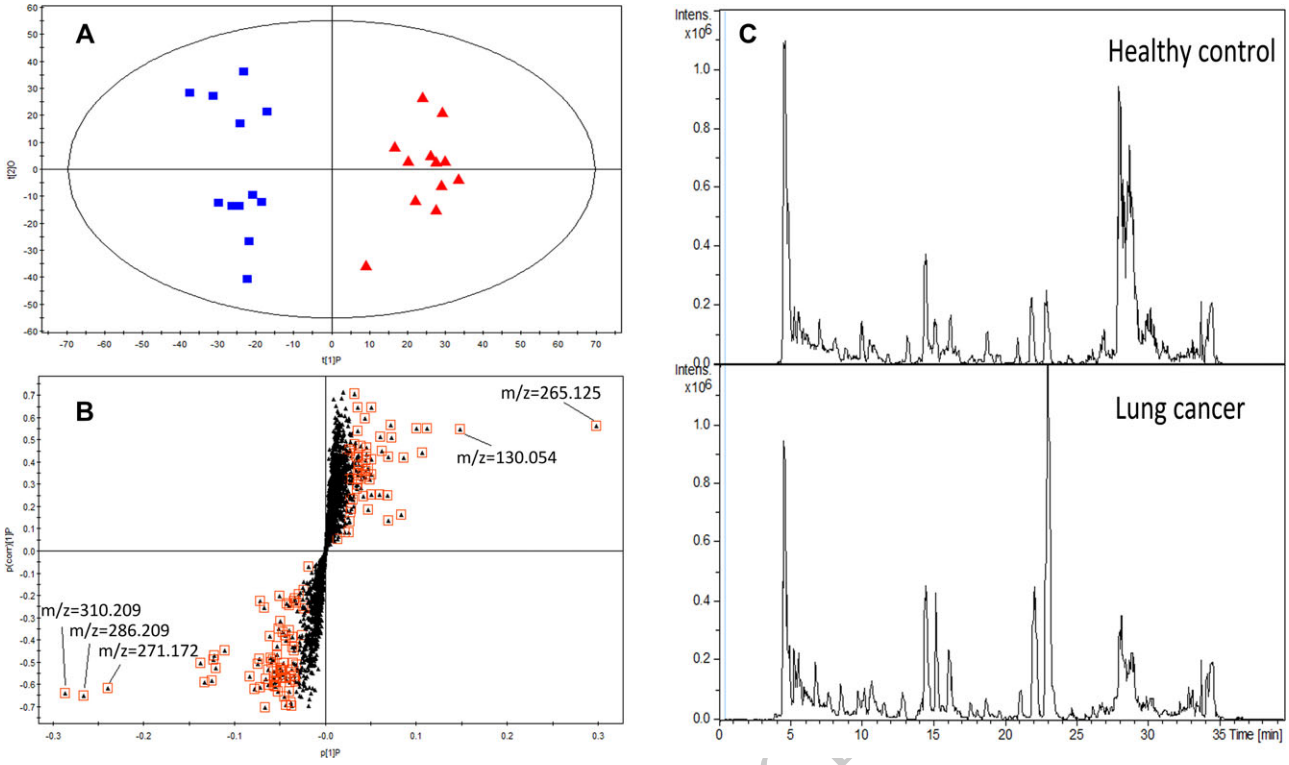

Figure 3. Orthogonal partial least squares-discriminant analysis (OPLS-DA) model results and typical base peak intensity (BPI) chromatograms. (A) OPLS-DA scores plot of healthy controls (■, blue squares) and lung cancer patients (▲, red triangles) based on urinary spectral data of pCEC-QTOF-MS (ESI+ mode). (B) S-plot based on the first component. The top 100 VIP variables were square-marked and the top 5 VIP variables were marked with *m/z* values. (C) Typical BPI hromatograms of urine samples from the healthy control and lung cancer groups.

plot and the S-plot of the orthogonal partial least squares-discriminant analysis model of 12 lung cancer patients and 12 healthy controls. Figure 3C displays the representative base peak intensity chromatograms in positive ion mode (ESI+) of pCEC-QTOF-MS obtained from a lung cancer patient and a healthy control. The model parameter for the explained variation (R2Y) was 0.944 and the predictive capability (Q2) was 0.654, which indicated that the model was satisfactory.

3.5 Discovery and identification of differential metabolites

Differential metabolites were screened and identified following the procedures described above. The variables with a VIP value ranked in the top 100, square marked in the S-plot (Fig. 3B), were selected for further screening. The top five VIP value variables were further marked with *m/z* values in the S-plot (Fig. 3B). Next, variables with large jack-knifed confidence intervals were excluded. Then Student's *t*-test was performed to exclude variables with $p > 0.05$. Subsequently, the elemental composition of the metabolites was calculated by the SmartFormula function of DataAnalysis software and mainly based on accurate mass and isotopic distribution. Based on the above procedures, a total of 15 differential metabolites were tentatively identified (Table 2).

Some approaches to lung cancer urinary metabolomics have recently been reported [37, 38]. N_6,N_6,N_6-trimethyl-L-lysine, an important precursor of carnitine, was reported as a potential biomarker of lung cancer by An [38]. Several acylcarnitines related to the fatty acid oxidation pathway were found as differential metabolites of lung cancer in this study. *O*-phosphotyrosine, uric acid, and series acylcarnitines, including the metabolite *m/z* 286 (acylcarnitine C8:1) [39] were also found in our previous global metabolomic study (manuscipt in preparation).

ESI is a so-called "soft ionization" technique [40], since there is very little fragmentation compared to atmospheric pressure chemical ionization (APCI) and electron ionization (EI) in most cases. However, for some metabolites with unstable structure, more fragmentation could be observed. More structural information can be gained from the multifragmentations but it is difficult to discriminate whether the ion is a co-eluted metabolite or just a fragment ion. As illustrated in Supporting Information Fig. S2, the pCEC-MS system had an additional selectivity due to the electroseparation mechanism. In this study, retention times of co-eluted ions in different separation mechanisms such as pCEC-MS, cHPLC-MS, and conventional HPLC-MS helped us determine whether the ion was a fragment ion. On the other hand, the fragmentations of auto MS/MS were applied as a complementary method to aid in this determination.

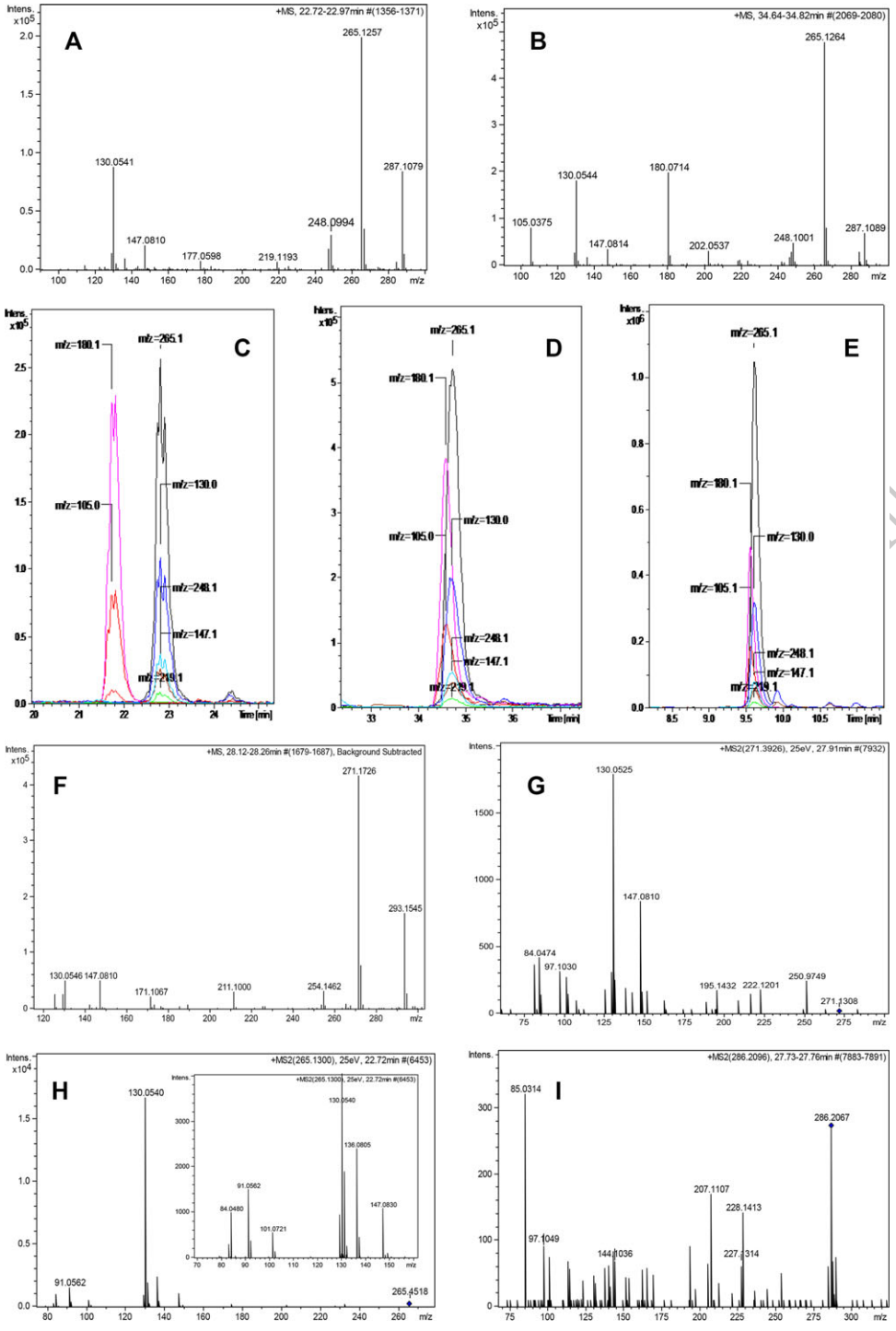

Figure 4. MS and MS/MS analysis of *m/z* 265, 271, and 286 ions. MS spectrum of the *m/z* 265 ion from a urine sample based on (A) pCEC-MS and (B) cHPLC-MS. Extracted ion chromatograms of the *m/z* 265 ion and related ions from a urine sample based on (C) pCEC-MS, (D) cHPLC-MS, and (E) HPLC-MS (separation conditions as in Supporting Information Table S3). (F) MS spectrum of the *m/z* 271 ion based on pCEC-MS. Auto MS/MS spectra of ions of (G) *m/z* 265, (H) *m/z* 271, and (I) *m/z* 286 based on pCEC-MS.

In this work, three interrelated differential metabolites (ions of *m/z* 265, 271, and 286) were found and identified. As shown in Fig. 4 and Table 2, the *m/z* 265 ion was identified as phenylacetylglutamine (PAGN) [41]. The ions of *m/z* 130, 147, 219, and 248 were attributed as fragment ions of PAGN according to the same retention times with PAGN in three different separation modes and the MS/MS fragmentation pattern. The ions of *m/z* 180 and 105 were determined as other metabolite(s) due to obvious separation resolution under pCEC mode, although they nearly co-eluted under cHPLC and HPLC mode (Fig. 4) and even appeared in the MS spectra of purified PAGN from urine [41].

Here we describe the identification of the *m/z* 271 ion. Web database search results of HMDB (http://www.hmdb.ca) and metlin (http://metlin.scripps.edu) indicated estrone as the most likely compound. However, the retention time and

Table 2. Summary of the differential urinary metabolites between lung cancer patients and healthy controls

No.	R_t (min)	*m/z* (Da)	VIP	PV1[a)]	PV2[b)]	FC[c)]	Candidate metabolites
1	4.17	189.1644	1.91	0.037	0.007	1.97	N_6,N_6,N_6-trimethyl-L-lysine
2	4.78	229.1251	5.13	0.016	0.015	2.04	Hydroxyprolyl-Proline
3	5.81	169.0407	4.51	0.033	0.021	1.52	Uric acid
4	6.76	147.0510	3.58	0.003		0.34	Unknown
5	9.17	262.0449	2.77	0.023	0.050	1.52	*O*-Phosphotyrosine
	9.34	182.0740	2.20	0.029		1.44	Fragment of ion *m/z* 262
6	22.19	243.1401	2.77	0.010	0.002	0.37	Acylglutamine C6:1
7	22.84	265.1251	13.10	0.015	0.015	1.59	PAGN
	22.82	248.0984	3.18	0.030		1.37	Fragment of ion *m/z* 265
	22.82	219.1179	2.31	0.003		1.59	Fragment of ion *m/z* 265
	22.85	147.0806	3.19	0.013		1.39	Fragment of ion *m/z* 265
	22.85	130.0538	7.06	0.011		1.47	Fragment of ion *m/z* 265
8	27.99	271.1725	10.83	0.005	0.001	0.48	Acylglutamine C8:1
	27.97	254.1460	2.38	0.010		0.61	Fragment of ion *m/z* 271
	27.98	147.0808	2.87	0.012		0.63	Fragment of ion *m/z* 271
	27.98	130.0546	3.51	0.005		0.57	Fragment of ion *m/z* 271
9	27.85	286.2087	13.74	0.001	0.001	0.49	Acylcarnitine C8:1
10	28.17	330.2353	3.34	0.043	0.033	0.59	Acylcarnitine C10:1+OH
11	28.41	310.2094	13.81	0.002	0.001	0.52	Acylcarnitine C10:3
12	29.07	356.2516	2.63	0.044	0.054	0.34	Acylcarnitine C13:1
13	29.11	336.2249	2.30	0.008	0.009	0.49	Acylcarnitine C12:4
14	29.31	302.2402	6.78	0.010	0.011	0.35	Acylcarnitine C9 (nonanoyl)
15	29.87	338.2408	2.70	0.007	0.018	0.47	Acylcarnitine C12:3
16	30.11	358.2672	6.15	0.006	0.004	0.31	Acylcarnitine C12:1+OH

a) PV1 is *p*-value obtained from Student's *t*-test.
b) PV2 is *p*-value obtained from Mann–Whitney *U* test.
c) FC is fold change, calculated as the average of lung cancer patients relative to the average of healthy controls.

MS/MS peaks of ion *m/z* 271 did not agree with the standard of estrone. By careful mass spectrum calibration, an accurate *m/z* of 271.1652 was obtained. The highest score result calculated by the SmartFormula function showed the formula was $C_{13}H_{23}N_2O_4$ (delta = 0.1 ppm, mSigma = 2.3, rdb = 3.5). The candidate compound had the same downregulated trend with acylcarnitine C8:1 in the lung cancer group, while it had a contrary trend compared to PAGN. However, the candidate's MS and MS/MS fragmentations were similar to PAGN. Based on the above information, the candidate was potentially identified as acylglutamine C8:1. Exact structure determination will require more information of the purified compound from urine samples.

The conjugation of glutamine, glycine, and taurine to some organic acids in the liver [42–44] is one of the liver phase II detoxification pathways, where specific substances are conjugated to metabolites to make them more water soluble or less harmful, easier to transport, and excretable from the body. Ions of *m/z* 265, 271, and 243 were identified as glutamine conjugates due to the same fragment ions of *m/z* 130 and 147 (Table 2). PAGN is one of the most common substances found in human urine and is known to form in liver with phenylacetyl-CoA [45]. Acylglutamine C8:1 and acylglutamine C6:1 are potentially phase II metabolites of specific fatty acids. Receiver-operating-characteristic analysis of acylglutamine C8:1 resulted in an area-under-curve value of 0.882 (Supporting Information Fig. S5). According to the above results, the pCEC-MS system proved to be a feasible analytical platform for the identification of distinctive metabolites (such as amino acid conjugates) as differential metabolites from urine samples.

4 Concluding remarks

An on-line gradient pCEC-QTOF-MS method has been developed for the analysis of urine metabolites. Three kinds of interfaces were designed and compared. The sheathless interface was selected for further experiments. The method was optimized and validated with mixed standards and urine samples, and successfully applied to lung cancer metabolomics. High separation efficiency was achieved using pCEC-MS. The different separation mechanism of pCEC helped to identify distinctive metabolites, demonstrating that the pCEC-QTOF-MS method might play an important role in future metabolomic studies.

This work was supported by National Natural Science Foundation of China (21175092, 21105064), National Important Instrument and Equipment Development Specific Projects (2011YQ150072, 2011YQ15007204, 2011YQ15007207, 2011YQ1500210), Shanghai Natural Science Foundation (12ZR1413600), and Science and Technology Department of Zhejiang Province Public Technology Research Program (2011C37014).

The authors have declared no conflict of interest.

5 References

[1] Knox, J. H., Grant, I. H., *Chromatogrphia* 1991, *32*, 317–328.

[2] Yan, C., Schaufelberger, D., Erni, F., *J. Chromatogr. A* 1994, *670*, 15–23.

[3] Yan, C., *Contemporary Microscale Separation Technology*, HNB Publishing, New York 2013.

[4] Griffiths, W. J., Wang, Y., *Chem. Soc. Rev.* 2009, *38*, 1882–1896.

[5] Banks, J. F., *Electrophoresis* 1997, *18*, 2255–2266.

[6] Warriner, R. N., Craze, A. S., Games, D. E., Lane, S. J., *J. Rapid Commun. Mass Spectrom.* 1998, *12*, 1143–1149.

[7] Zheng, J., Shamsi, S. A., *Anal. Chem.* 2003, *75*, 6295–6305.

[8] Lee, E. D., Mück, W., Henion, J. D., Covey, T. R., *Biomed Environ Mass Spectrom* 1989, *18*, 844–850.

[9] Aturki, Z., D'Orazio, G., Rocco, A., Bortolotti, F., Gottardo, R., Tagliaro, F., Fanali, S., *Electrophoresis* 2010, *31*, 1256–1263.

[10] Desiderio, C., Fanali, S., *J. Chromatogr. A* 2000, *895*, 123–132.

[11] Bragg, W., Norton, D., Shamsi, S. A., *J. Chromatogr. B* 2008, *875*, 304–316.

[12] Chen, C. J., Chang, C. H., Her, G. R., *J. Chromatogr. A* 2007, *1159*, 22–27.

[13] Chen, C. J., Wang, C. W., Her, G. R., *J. Sep. Sci.* 2011, *34*, 2538–2543.

[14] Ramautar, R., Somsen, G. W., de Jong, G. J., *Electrophoresis* 2009, *30*, 276–291.

[15] Ramautar, R., Mayboroda, O. A., Somsen, G. W., de Jong, G. J., *Electrophoresis* 2011, *32*, 52–65.

[16] Ramautar, R., Somsen, G. W., de Jong, G. J., *Electrophoresis* 2013, *34*, 86–98.

[17] Ramautar, R., Busnel, J. M., Deelder, A. M., Mayboroda, O. A., *Anal. Chem.* 2012, *84*, 885–892.

[18] Behnke, B., Bayer, E., *J. Chromatogr. A* 1994, *680*, 93–98.

[19] Wu, J. T., Huang, P., Li, M. X., Lubman, D. M., *Anal. Chem.* 1997, *69*, 2908–2913.

[20] Schmeer, K., Behnke, B., Bayer, E., *Anal. Chem.* 1995, *67*, 3656–3658.

[21] Liang, Z., Duan, J., Zhang, L., Zhang, W., Zhang, Y., Yan, C., *Anal. Chem.* 2004, *76*, 6935–6940.

[22] Liang, Z., Zhang, L., Duan, J., Yan, C., Zhang, W., Zhang, Y., *Electrophoresis* 2005, *26*, 1398–1405.

[23] Huang, P., Wu, J. T., Lubman, D. M., *Anal. Chem.* 1998, *70*, 3003–3008.

[24] Lu, M., Zhang, L., Feng, Q., Xia, S., Chi, Y., Tong P., Chen G., *Electrophoresis* 2008, *29*, 936–943.

[25] Lu, M., Zhang, L., Qiu, B., Feng, Q., Xia, S., Chen, G., *J. Chromatogr. A* 2008, *1193*, 156–163.

[26] Lu, M., Zhang, L., Li, X., Lu, Q., Chen, G., Cai, Z., *Talanta* 2010, *81*, 1655–1661.

[27] Cheng, J., Zhang, L., Lu, Q., Lu, M., Chen, Z., Chen, G., *Electrophoresis* 2010, *31*, 1991–1997.

[28] Johannesson, N., Olsson, L., Bäckström, D., Wetterhall, M., Danielsson, R., Bergquist, J., *Electrophoresis* 2007, *28*, 1435–1443.

[29] Que, A. H., Konse, T., Baker, A. G., Novotny, M. V., *Anal. Chem.* 2000, *72*, 2703–2710.

[30] Kato, M., Onda, Y., Sekimoto, M., Degawa, M., Toyo'oka, T., *J. Chromatogr. A* 2009, *1216*, 8277–8282.

[31] Xie, G., Su, M., Li, P., Gu, X., Yan, C., Qiu, Y., Li, H., Jia, W., *Electrophoresis* 2007, *28*, 4459–4468.

[32] Zhang, H., Wang, Y., Gu, X., Zhou, J., Yan, C., *Electrophoresis* 2011, *32*, 340–347.

[33] Wiklund, S., Johansson, E., Sjöström, L., Mellerowicz, E. J., Edlund, U., Shockcor, J. P., Gottfries, J., Moritz, T., Trygg, J., *Anal. Chem.* 2008, *80*, 115–122.

[34] Jansson, J., Willing, B., Lucio, M., Fekete, A., Dicksved, J., Halfvarson, J., Tysk, C., Schmitt-Kopplin, P., *PLoS One* 2009, *4*, e6386.

[35] Kim, Y., Koo, I., Jung, B. H., Chung, B. C., Lee, D., *BMC Bioinformatics* 2010, *11*(Suppl 2), S4.

[36] Pucci, V., Di Palma, S., Alfieri, A., Bonelli, F., Monteagudo, E., *J. Pharm. Biomed. Anal.* 2009, *50*, 867–871.

[37] Yang, Q., Shi, X., Wang, Y., Wang, W., He, H., Lu, X., Xu, G., *J. Sep. Sci.* 2010, *33*, 1495–1503.

[38] An, Z., Chen, Y., Zhang, R., Song, Y., Sun, J., He, J., Bai, J., Dong, L., Zhan, Q., Abliz, Z., *J. Proteome Res.* 2010, *9*, 4071–4081.

[39] Yang, S., Minkler, P., Hoppel, C., *J. Chromatogr. B* 2007, *857*, 251–258.

[40] Fenn, J. B., Mann, M., Meng, C. K., Wong, S. F., Whitehouse, C. M., *Science* 1989, *246*, 64–71.

[41] Fukui, Y., Kato, M., Inoue, Y., Matsubara, A., Itoh, K., *J. Chromatogr. B* 2009, *877*, 3806–3812.

[42] Bridges, J. W., Evans, M. E., Idle, J. R., Millburn, P., Osiyemi1, F. O., Smith, R. L., Williams, R. T., *Xenobiotica* 1974, *4*, 645–652.

[43] Williams, R. T., *Environ. Health Perspect.* 1978, *22*, 133–138.

[44] Emudianughe, T. S., Caldwell, J., Smith, R. L., *Xenobiotica* 1987, *17*, 823–828.

[45] Webster, L. T., Siddiqui, U. A., Lucas, S. V., Strong, J. M., Mieyal, J. J., *J. Biol. Chem.* 1976, *251*, 3352–3358.

Address：489 Songtao Road, C01, Zhangjiang High-tech Park, Pudong, Shanghai 201203, P.R. China
E-Mail：info@unimicrotech.com，lemonyu@unimicrotech.com
Website：www.unimicrotech.com

